SAMPLING STRATEGIES AND RESOLUTION IN LIMITED DATA CONE-BEAM TOMOGRAPHY

F. Noo

University of Liège, Belgium
University of Utah, USA

R. Clackdoyle

University of Utah, USA

1. INTRODUCTION

This paper concerns cone-beam tomography from limited data. Cone-beam tomography is a technique used to visualize the interior of a three-dimensional (3-D) object in a non-invasive way. This technique involves two steps. In the first step, measurements called cone-beam projections are taken. In the second step, digital signal processing techniques are used to process the measurements to form a 3-D image.

The 3-D image represents a function $f(\underline{x})$ which associates each voxel $\underline{x}$ in the object with the value of a physical quantity. In x-ray imaging, this quantity is the x-ray attenuation factor which roughly corresponds to the density of the object. In single photon emission computed tomography (SPECT), the physical quantity is the concentration of a radioactive tracer injected into the 3-D object (the patient).

A cone-beam projection is a 2-D set of integrals of $f(\underline{x})$ measured along lines which diverge from a given vertex point $\underline{a}$. In x-ray imaging, the vertex point is an x-ray source and the projection is usually called a radiograph. The object lies between the x-ray source and an area detector as shown in figure 1. Physically, the x-rays travel along lines which diverge from $\underline{a}$ and undergo a net attenuation depending on the densities encountered in the object. The cone-beam projection is the set of intensity losses (integrals of $f(\underline{x})$) observed along each line. These intensity losses are measured on the area detector; they form a 2-D image (radiograph) of the 3-D object under study.

In SPECT, the area detector is replaced by a gamma camera with a collimator. The gamma camera is used to count photons; the sum of photons emitted in a given direction is proportional to a line integral of $f(\underline{x})$. The collimator restricts the photons to specific lines by an arrangement of cylindrical holes. To obtain a cone-beam projection, the holes are oriented towards a single focal point in space. The vertex point $\underline{a}$ is the collimator focal point.

With ideal (noiseless) projections, the imaging capabilities of a cone-beam tomographic system are determined by the locations of the vertices relative to the object. Most works on cone-beam tomography are based on Tuy's condition [1] which requires the vertices to be finely sampled along certain kinds of curves in space. This condition ensures accurate tomographic reconstructions but requires many (typically hundreds of) projections. If data collection is slow however, it may not be possible to acquire enough projections. Also, sampling the projections along an appropriate vertex curve is not always possible due to physical constraints. One example is imaging during interventional surgery. For such an application, only a small number of projections can be considered to ensure fast image update. Also, the physical constraints of a crowded operating room will preclude certain locations for taking measurements. Limited data cone-beam tomography refers to the situation where ideal tomography is not possible due to insufficient or inappropriately placed cone-beam projections.

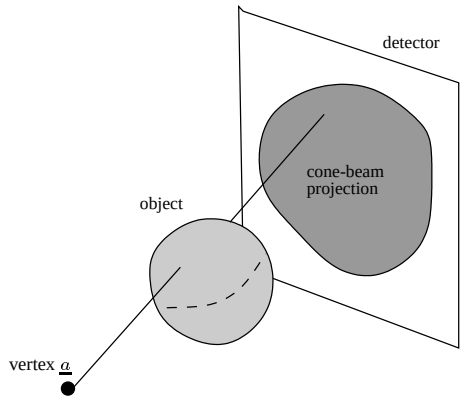

Fig. 1. Cone-beam projection for a given vertex $\underline{a}$. The cone-beam projection is the 2-D set of integrals of $f(\underline{x})$ measured along the lines which diverge from $\underline{a}$.

Given time and environment constraints, it is important for the scanner manufacturer to know where the cone-beam projections should be collected to best achieve a given imaging objective. By avoiding the measurement of projections which have a low information content for the recovery of the features of interest in $f(\underline{x})$, the scanner performance can be optimized.

In limited data cone-beam tomography the fundamental question is: given a set of projections, what is the inherent tomographic capability of the system ? Another question immediately follows: how should the projections be processed to achieve this resolution capability ?

The literature on vertex sampling and inherent tomographic capability for cone-beam tomography is very meagre. In 1994, Barrett and Gifford published a work on vertex sampling for the helical vertex path and used the concept of a Fourier cross-talk matrix to compare different sampling strategies [2]. Their work readily generalizes to other curves, and to non-uniform sampling schemes but it treats the object in a uniform way and does not account for local variations in tomographic recoverability. A somewhat related work of Quinto [3] discusses information contained in cone-beam projections using the rigorously-defined concepts of visible and invisible singularities (e.g object boundaries). Some of the ideas of our work are based on these concepts. However,

Quinto's work makes no attempt to discuss the tomographic recoverability of $f(\underline{x})$, and in the limit of a Tuy-complete curve with fine vertex sampling, it would only predict that all *singularities* of $f(\underline{x})$ are visible. Looking further afield, there are established methods [4, 5] to determine optimal sampling schemes in classical (parallel-beam and fan-beam) tomography, and Desbat [6] has applied these methods to one particular cone-beam case. For cone-beam tomography, these methods require vertex sampling along a suitable (Tuy) path, and can only indicate optimal *uniform* sampling. These requirements are far too restrictive for our purposes.

For the issue of image reconstruction, only the work of Noo *et al.* [7] is relevant to a geometry of unordered (not along a curve) vertex locations. Iterative methods might also be applied, but regularization and stopping criteria would be hard to establish without prior information of what features can be recovered in principle.

This paper addresses the prediction of tomographic capabilities of limited-data cone-beam tomographic systems. We introduce the notion of "local directional resolution" to predict these capabilities and illustrate its usefulness in a simulation of SPECT breast imaging.

2. RESOLUTION CAPABILITIES

2.1. Problem statement

The problem we are interested in is the characterization of the "tomographic capability" of a limited set of cone-beam measurements. Given N cone-beam projections measured at vertices $\underline{a}_i$, $i = 1, \ldots, N$, we aim at characterizing what can be and what cannot be recovered in the 3-D object using tomographic reconstruction.

Some assumptions are made to simplify the problem. We consider that the area detector has infinite resolution and the projections are non-truncated. Figure 1 gives the illustration of such a projection. Non-truncation means that the area detector is large enough to intercept any line which diverges from the vertex and goes through the object. This condition is unfortunately rarely met in practice and constitutes therefore a strong limitation in our study. On the other hand, infinite detector resolution, although not physically realizable, is a weak assumption because many area detectors currently have submillimeter resolution.

2.2. Local directional resolution

In this work, the tomographic capability of a set of cone-beam measurements is characterized in terms of resolution. For cone-beam systems, resolution depends on position $\underline{x}$ and orientation $\underline{\theta}$. This statement can be understood from figure 2 where we show the differences occuring in the cone-beam projection of a simple object when changing its orientation and position.

To evaluate the resolution capability at point $\underline{x}$ in direction $\underline{\theta}$, we introduce the "local directional resolution" function $R(\underline{x}, \underline{\theta})$; $R(\underline{x}, \underline{\theta})$ is the smallest resolvable distance at location $\underline{x}$ in direction $\underline{\theta}$. By definition, $R(\underline{x}, \underline{\theta})$ can vary from 0 to $+\infty$. When the projections are known for all vertices on a curve satisfying Tuy's condition, exact reconstruction is possible and $R(\underline{x}, \underline{\theta}) = 0$. At the other extreme, we have $R(\underline{x}, \underline{\theta}) = +\infty$ when $N = 1$ and $\underline{\theta}$ is parallel to the line connecting $\underline{x}$ to the unique vertex. This situation was illustrated in figure 2 (right).

For a cone-beam configuration of N vertices, we suggest

$$R(\underline{x}, \underline{\theta}) \quad = \quad \text{constant} \times \min\left\{ \tan \psi_i \right\}_{i=1,\ldots,N} \qquad (1)$$

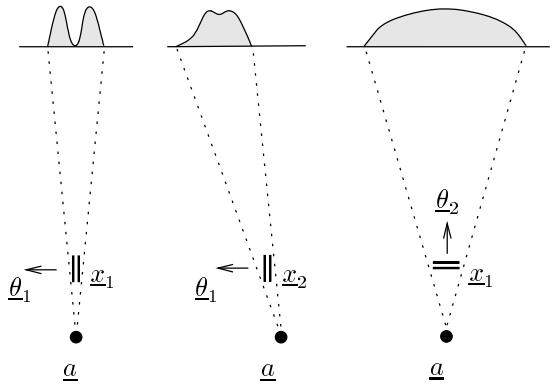

Fig. 2. Resolution and cone-beam projections. For cone-beam systems, resolution depends on position $\underline{x}$ and orientation $\underline{\theta}$. The figure illustrates the situation for one vertex. The object consists of two parallel disks. Only the details which are visible in the projection can be recovered. Left: the disk separation is clearly visible. Middle: by changing the position of the object, the resolution is degraded. Right: by changing the object orientation, the disk separation becomes invisible.

where

$$\sin \psi_i = \frac{|(\underline{a}_i - \underline{x}) \cdot \underline{\theta}|}{||\underline{a}_i - \underline{x}||} \,. \qquad (2)$$

Geometrically, ψ_i is the angle at $\underline{x}$ between $\underline{a}_i$ and the plane with normal $\underline{\theta}$.

3. EVALUATION

In this section, we use the local directional resolution function $R(\underline{x}, \underline{\theta})$ of equation (1) to predict the tomographic capabilities of a SPECT breast imaging system which would use a pinhole collimator for data acquisition.

3.1. Cone-beam configuration

Figures 3 and 4 illustrate the SPECT breast imaging system under investigation. We consider that cone-beam projections are collected for vertex positions lying on three parallel semi-circles centered on the right breast. The number of vertices per semi-circle is 12. So, there are 36 projections in total. Figure 4 illustrates the arrangement of the vertices in space.

3.2. Resolution capability

The local directional resolution of the cone-beam system is evaluated using test-objects built from disks. Each object is obtained by stacking up three disks one above the other (see figure 4). The diameter and thickness of the disks are 7 mm and 1 mm, respectively. The gap between two disks is 2 mm. To test the resolution at point $\underline{x}$ in direction $\underline{\theta}$, we place the test object at $\underline{x}$ with its symmetry axis along $\underline{\theta}$.

As shown in figure 4, five test-objects are placed in the breast, both inside and outside the hemisphere. Conventional cone-beam theory would predict reasonable tomography only for objects 1 and 5. The value of $R(\underline{x}, \underline{\theta})$ was evaluated for each of these test-objects using formula (1). The results are reported in table 1. According

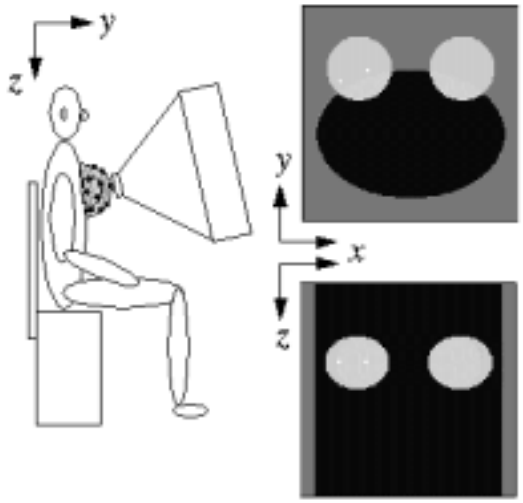

Fig. 3. SPECT breast imaging system using a pinhole collimator. The pinhole position corresponds to the vertex location. Magnification around the right breast shown on figure 4.

test-object	1	2	3	4	5
$R(\underline{x},\underline{\theta})$	0	8.5	7.5	40	6.8

Table 1. Values of $R(\underline{x},\underline{\theta}) = 100 \times \min\{\tan\psi_i\}_{i=1,\ldots,N}$ (formula (1)) for the 5 test-objects in figure 4.

to this table, object 1 should be easier to recover than the other objects, objects 2, 3 and 5 should be similarly recoverable, and object 4 should be much more difficult to recover. To verify these results, we performed a reconstruction of the breast phantom using the algorithm described in [7]. The result, shown in figure 5, confirmed our prediction.

4. DISCUSSION

In this work, we presented results concerning the prediction of the tomographic capabilities of a limited data cone-beam system. We introduced the notion of local directional resolution $R(\underline{x},\underline{\theta})$ to predict how well structures can be separated at a point $\underline{x}$ in a given direction $\underline{\theta}$. A simulation of a SPECT breast imaging system was performed to verify the predictions of our formula for $R(\underline{x},\underline{\theta})$. The results were conclusive. Further work is needed to relate $R(\underline{x},\underline{\theta})$ to a measure of the image quality achievable at $\underline{x}$ in the direction $\underline{\theta}$. Note that the reconstruction algorithm used in this experiment was not designed to obtain optimal resolution results. Further work is also needed to design an algorithm which would achieve that goal.

5. ACKNOWLEDGMENTS

This work was partially supported by the National Institutes of Health, grant number R21 CA 82843. The work of F. Noo was supported by the Belgian National Fund for Scientific Research.

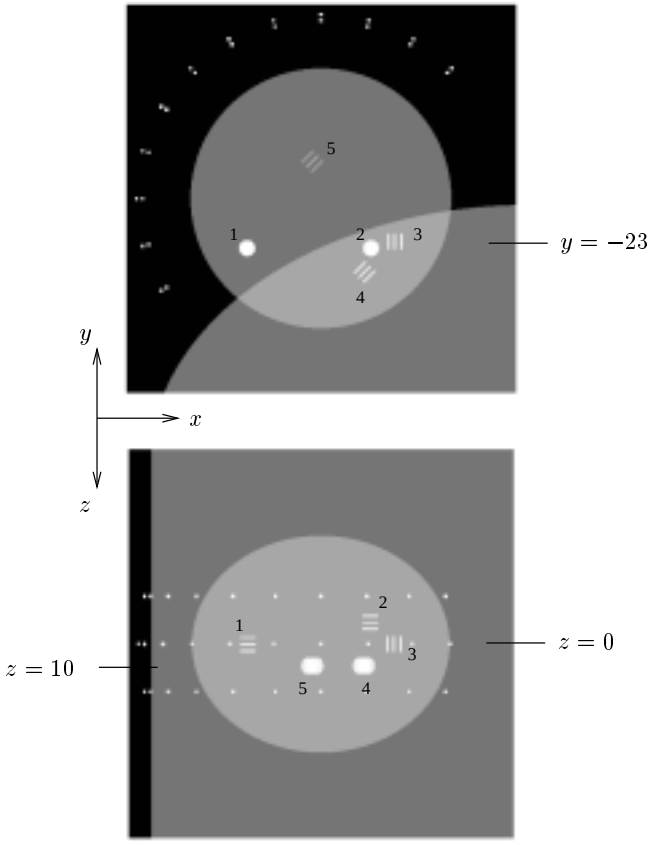

Fig. 4. Vertex locations and test-objects for tomographic imaging of the right breast. Torso shown for illustration only. Uniform breast activity was simulated, with 5 high intensity test objects placed as shown.

6. REFERENCES

[1] H. Tuy, "An inversion formula for cone-beam reconstruction", SIAM J. Appl. Math., 43, 1983, 546-552.

[2] H. H. Barrett, H. Gifford, "Cone-beam tomography with discrete data sets", Physics in Medicine and Biology, 39, 1994, 451-476.

[3] E. T. Quinto, "Singularities of the x-ray transform and limited data tomography in $\mathbb{R}^2$ and $\mathbb{R}^3$", SIAM J. Math. Anal., 24(5), 1993, 1215-1225.

[4] P. A. Rattley, A. G. Lindgren, "Sampling the 2-D Radon transform", IEEE Trans. ASSP, 29, 1981, 994-1002

[5] F. Natterer, "Sampling in fan-beam tomography", SIAM J. Appl. Math. 53(2), 1993, 358-380.

[6] L. Desbat, "Échantillonnage parallèle efficace en tomographie 3D", C. R. Acad. Sci. Paris, 324(I), 1997, 1193-1199.

[7] F. Noo, R. Clack, M. Defrise, "Cone-beam reconstruction from general discrete vertex sets using Radon rebinning algorithms", IEEE Transactions on Nuclear Science, 44(3), 1997, 1309-1316.

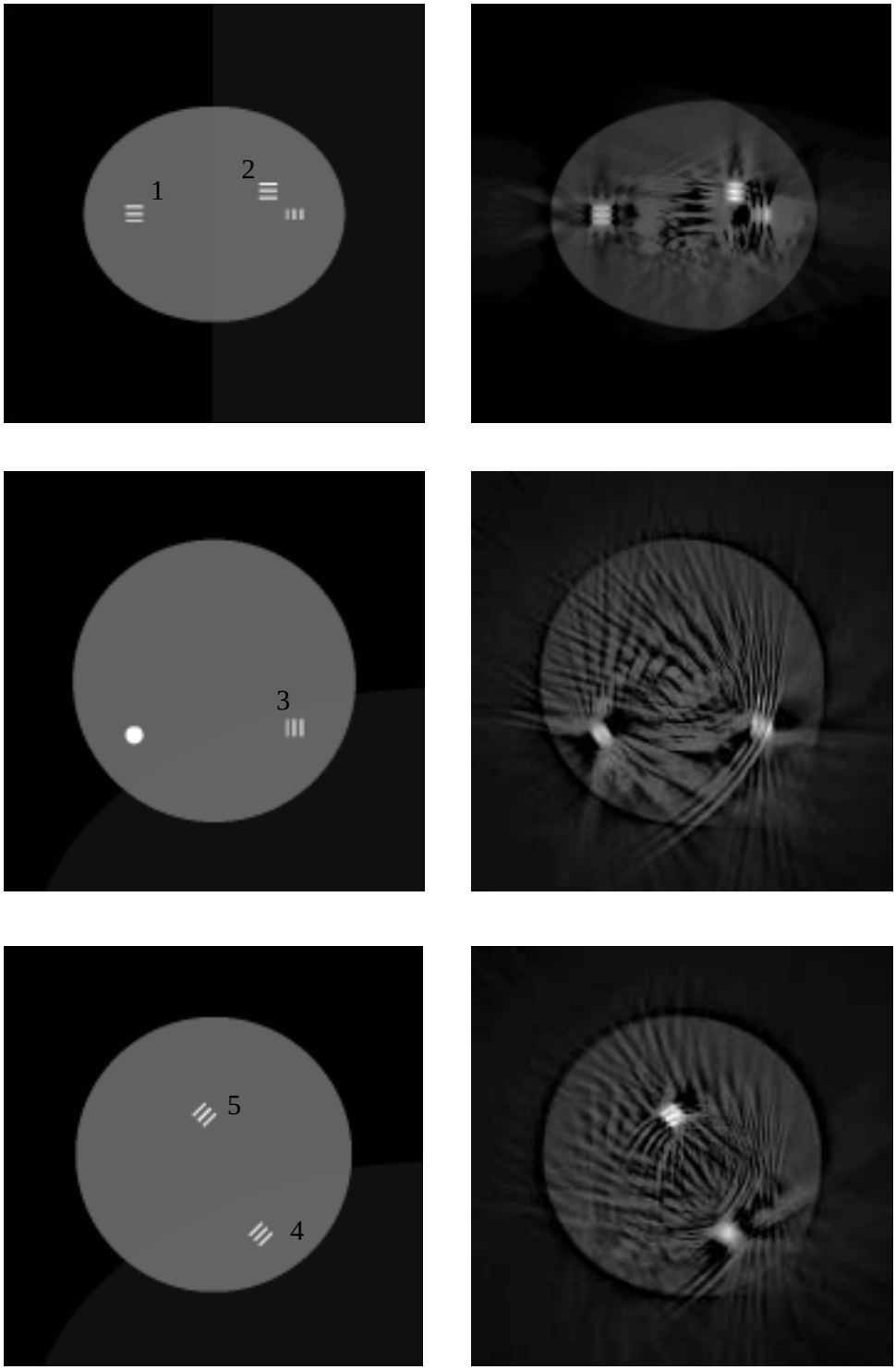

Fig. 5. Reconstruction results. Top row: slice $y = -23$. Middle row: slice $z = 0$. Bottom row: slice $z = 10$. The separation between the disks is well-recovered for the test-objects 1,2,3, and 5. The cone-beam configuration is not suitable for the reconstruction of object 4. The contours of object 1 are better defined than those of objects 2,3 and 5 in the reconstruction.